IEEE Access
Multidisciplinary | Rapid Review | Open Access Journal

Received 13 December 2023, accepted 10 January 2024, date of publication 18 January 2024, date of current version 26 January 2024.

Digital Object Identifier 10.1109/ACCESS.2024.3355451

RESEARCH ARTICLE

Millimeter-Wave Channel Estimation Based on 2-D Beamspace MODE Method

LI HOU, JING WU, AND WEI HENG, (Member, IEEE)
National Mobile Communications Research Laboratory, Southeast University, Nanjing 210096, China
Corresponding author: Wei Heng (wheng@seu.edu.cn)

This work was supported in part by the National Natural Science Foundation of China under Grant 61771132.

ABSTRACT The directions and gains of the paths with significant power can reconstruct mm-wave channel estimation, attributed to spatial sparsity resulting from severe propagation loss. Leveraging this feature, the two-dimensional beamspace method of direction estimation (2-D BMODE) is developed to estimate the path directions, including angles of departure and arrival. The least-squares(LS) method is then employed to estimate the path gains. Different from the beamspace two-dimensional multiple signal classification (MUSIC) method, the method proposed in this paper significantly ruduces computational complexity without spectral search. Moreover, the DODs and DOAs can be paired automatically by reduced-dimension(RD) MUSIC. Meanwhile, the performance of this method deteriorates when the covariance matrix of gains isn't of full column rank. This paper also enhances the performance using spatial smoothing technique and oblique projecting to overcome the influence of rank deficiency. The 2-D BMODE method, as illustrated in this paper, outperforms in terms of both unity in computational complexity and estimation accuracy. Numerical simulations validate the advantages and demonstrate the method can serve as a superior alternative.

INDEX TERMS Channel estimation, two-dimensional MODE, hybrid beamforming, spatial smoothing, oblique projection.

I. INTRODUCTION

Millimeter wave (mm-wave) communication has received a significant amount of attention over the last several decades, particularly focusing on multiple-input multiple-output(MIMO) system [1], [2], [3], [4]. The mm-wave has a shorter wavelength, offering unique advantages, such as a much smaller physical size occupied by the antenna array [5]. Simultaneously, a key feature of mm-wave systems is the more severe propagation loss compared to microwave systems. Consequently, the traditional MIMO channel models can not describe the spatial sparsity of the mm-wave channel, primarily concentrated in a few dominant paths because of rich scattering. Alternately, mm-wave channels can be parametrically modeled based on the path angles of departure/arrival (AoD/AoA) and the corresponding path gains. Apparently, the mm-wave channel estimation problem transforms into one of estimating the path directions and gains, rather than estimating the MIMO channel matrix [6], [7], [8].

For the purpose of overcoming the shortcomings of mm-wave communications and leveraging the gains provided by multiple antennas, beamforming technology is widely considered [9]. Hybrid beamforming shows great promise in reaching a balance between rate enhancement and power saving. Considering the mm-wave signals, which are highly directional and consist of several significant components, a straightforward and low-complexity approach to mm-wave channel estimation is to search in angular space by adjusting the direction of beamforming [10], [11], [12]. Nevertheless, the exhaustive search may face hindrance due to the high training overhead in practice. To avoid an exhaustive beam search, [11] and [12] propose a hierarchical multi-beam search scheme that divides the beam training into multiple phases. First, multiple wide beams cover all angular spaces, and the transmitters select the angular range of great significance to the objective. Subsequently, the angular range previously fed back to transmitters is used to form

The associate editor coordinating the review of this manuscript and approving it for publication was Li Zhang.

narrow beams. The above process is repeated until the desired resolution is attained.

In contrast to beam training methods, [7] addresses the mm-wave channel estimation problem using an orthogonal matching pursuit(OMP) algorithm. The OMP algorithm ensures that the residuals are orthogonal to current and all previously selected atoms, improving the algorithm's sparse reconstruction performance. In addition, in [13] and [14], a significant number of MIMO channel estimation problems are also addressed using compressed sensing (CS)-based methods. These CS-based methods treat sparse multipath channel estimation as a problem of sparse recovery. Due to the spatial sparsity of the mm-wave channels, a small fraction of the gain coefficients are non-zero, which is essential for path directions. The sparse recovery methods aim to recover the non-zero gain coefficients, providing an estimation of the path direction while minimizing the training overhead.

Literature [15] exploits the inherent sparsity of mm-wave channels, formulating the channel estimation problem as atomic norm minimization to enhance sparsity in the continuous DoAs and DoDs. In order to address the channel estimation problem posed by these formulas, which stem from pilot-assisted and data-aided channel estimators, a computationally efficient conjugate gradient descent method, originating from nonconvex factorization, is developed to restricted the search space to low-rank matrices in [15].

In contrast to the aforementioned work, [16] addresses the mm-wave estimation problem using the spatial spectral estimation (SSE) method. Particularly, in [17] and [18], the AoDs/AoAs are estimated using 2-D BMUSIC and 2-D ESPRIT schemes, respectively. When the AoDs and AoAs are fixed, the path gains are estimated by using the LS method. The detailed discussion regarding conditions to avoid spectrum ambiguity and maximum number of resolvable path directions can be found in [17]. Therefore, we skip it to avoid redundancy. The previous schemes are typically based on the uniform linear arrays (ULAs). However, unlike for the ULAs, larger array apertures can be achieved by fewer array elements using co-prime arrays, which is beneficial to improve the performance of arrival direction estimation, contributing to the estimation performance of AoAs and AoDs [19]. In [19], for each path direction, multiple peaks are generated in the spatial spectrum of each subarray. An arbitrary peak is then searched by selecting over any finite sector, allowing recovery of the remaining peaks. The correct path direction is obtained by comparing the peaks of the two subarrays when the common peaks appear.

In this paper, the MODE method, adopted for mm-wave channel estimation, has been previously used to estimate the AoDs for MIMO system in [20]. Nevertheless, this literature only considers the single-antenna case, where the transmitter and receiver do not need to consider beamforming. In contrast to existing work, hybrid beamforming structures are incorporated into mm-wave MIMO systems to facilitate channel estimation. The main contributions of this paper can be summarized as follows.

1) The conventional beamspace MUSIC algorithm is able to obtain the AoDs and AoAs by spectral peak search, but this method tends to be computationally intensive. The 2-D BMODE algorithm developed in this paper calculates the desired angles through iteration, significantly reducing the computational cost. Additionally, the use of the RD MUSIC algorithm to transform the two-dimensional search into a one-dimensional search also enhances computational efficiency.
2) When paths in the mm-wave channel with idential gain values, accurately and completely sreaching the AoDs and AoAs becomes challenging due to the rank deficiency of the covariance matrix of gains. The use of an oblique projector and forward-backward spatial smoothing can improve the accuracy of the acquisition angle. In order to minimize the influence of beamformers, the discrete fourier transform (DFT) beamformers are designed for use in the proposed channel estimator. These beamformers are commonly employed in the hybrid beamforming structure of mm-wave communication systems and don't lead to spectrum ambiguity. The detailed analysis is provided in [17].

The remainder of the paper is organized as follows. Section II presents the system model, establishing the basis for subsequent channel estimation methods. In Section III, we introduce the 2-D BMUSIC method and present the 2-D BMODE and RD-MUSIC algorithms to reduce the spectral peak search time. Oblique projector and forward-backward apatial smoothing are employed to handle non-orthogonal resulting from the rank deficiency of the gains matrix. The complexity is analyzed in Section IV. Section V illustrates the performance using computer simulation, and Section VI concludes the paper.

Notations: $\mathbf{I}_K$ and $\mathbf{0}_{M\times K}$ denote a $K \times K$ identity matrix and an $M \times K$ zero matrix, respectively; a, $\mathbf{a}$ and $\mathbf{A}$ indicate a scalar, a column vector, and a matrix, respectively; $\mathbf{A}^*$, $\mathbf{A}^T$, $\mathbf{A}^\dagger$ and $\mathbf{A}^H$ denote the conjugate, transpose, Moore-Penrose inverse and conjugate transpose of $\mathbf{A}$, respectively; $\mathbf{A}_{[:,i]}$ is the i^{th} column of $\mathbf{A}$, and diag$\{\mathbf{a}\}$ is a diagonal matrix with the elements of $\mathbf{a}$ on the diagonal; $\otimes$ and $\odot$ denote the Kronecker product and Khatri-Rao product, respectively; and $\|\mathbf{A}\|_{\text{F}}$ denotes the Frobenius norm of $\mathbf{A}$.

II. SIGNAL MODEL

Fig.1 illustrates the employed hybrid analog/digital beamforming, a promising scheme crucial for reducing the hardware cost of millimeter wave communication system [6]. The system has $N_t = DN_1$ and $N_r = DM_1$ antennas at the transmitter and receiver, respectively, where D is the number of sub-arrays. Furthermore, the numbers of RF chains at the transmitter and receiver are $M_t = DD_t$ and $M_r = DD_r$, respectively. Within the hybrid structure, data streams are

mapped to different antennas through an analog precoder $\mathbf{F} \in \mathbb{C}^{N_t \times M_t}$ $(M_t \leq N_t)$. The same hybrid structure is used at the receiver, where received signals are first processed by an analog combiner $\mathbf{W} \in \mathbb{C}^{N_r \times M_r}$ $(M_r \leq N_r)$. In this paper, we are only concerned about the mm-wave channel estimation problem.

For mm-wave channels, only limited information on the path parameters is required to determine the mm-wave model, as the dramatic path loss of mm-wave transmission severely limits the number of transmission paths in the channel. Therefore, the ray-tracing model is commonly used in mm-wave communication systems. The ray-tracing model describes the multipath channel based on various parameters of the transmission path in the wireless channel, so it is a parametric channel model [6]. Assuming the existence of K clusters, with each cluster contributing to the resolved path, the channel model can be written as [6]

$$\mathbf{H}(q) = \sum_{k=1}^{K} \alpha_k(q)\, \mathbf{a}_r(\theta_k)\mathbf{a}_t^H(\phi_k) \in \mathbb{C}^{N_r \times N_t}, \tag{1}$$

where $\mathbf{a}_r(\cdot)$ and $\mathbf{a}_t(\cdot)$ are the antenna array response at the receiver and transmitter, respectively. Assuming that the antenna arrays are installed in the horizontal direction, $\mathbf{a}_t(\phi_k) = \left[1, e^{j\rho d \sin\phi_k}, \ldots, e^{j\rho d(N_t-1)\sin\phi_k}\right]^T$ and $\mathbf{a}_r(\theta_k) = \left[1, e^{j\rho d \sin\theta_k}, \ldots, e^{j\rho d(N_r-1)\sin\theta_k}\right]^T$. Here, $\rho = \frac{2\pi}{\lambda}$, both for transmitter and receiver, d is set to $\frac{\lambda}{2}$, we denote ϕ_k and θ_k as the departure and arrival directions of the k^{th} path, $\alpha_k(q) \overset{i.i.d}{\sim} \mathcal{CN}\left(0, \sigma_k^2\right)$is the fading gain of the k^{th} path, and q is used to index the time block during which the mm-wave channel is considered fixed. In (1), for the sake of facilitating the description and analysis, we assume that the channel is caused only by the path gain $\{\alpha_k(q)\}_{k=1}^K$, with the path angles remaining constant. This assumption of time variation is based on the mm-wave channel measurements in [21], indicating that the central angle of the cluster belongs to a large-scale fading, whereas the path gain belongs to a small-scale fading. For ease of symbolic representation, (1) can be compactly rewritten in the form of

$$\mathbf{H}(q) = \mathbf{A}_R \mathbf{\Lambda}_\alpha(q) \mathbf{A}_T^H \tag{2}$$

where $\mathbf{\Lambda}_\alpha(q) = \text{diag}\{\alpha_1(q), \ldots, \alpha_K(q)\} \in \mathbb{C}^{K\times K}$, $\mathbf{A}_T = [\mathbf{a}_t(\phi_1)\ldots\mathbf{a}_t(\phi_K)] \in \mathbb{C}^{N_t\times K}$, and $\mathbf{A}_R = [\mathbf{a}_r(\theta_1)\ldots\mathbf{a}_r(\theta_K)] \in \mathbb{C}^{N_r\times K}$.

III. CHANNEL ESTIMATION PROCEDURE

The 2-D BMODE method, developed to estimate the path directions, relies on the matrix factorization of the covariance matrix. Therefore, we first need to obtain the received signal. Once the estimated angles are acquired, we then use the LS method to estimate the path gains. In the above process, attention must be paid to the case of rank defificiency.

A. THE RECEIVED SIGNAL EXPRESSION

We assume that the pilot signal transmitted at the m^{th} $(m = 1, \ldots, M_t)$ RF chain during one time block is defined as [17]

$$p_m(t) = \sqrt{\frac{E}{M_t}}\varphi(t - (m-1)T) \tag{3}$$

where E represents the transmit power assigned equally for each pilot signal, and $\varphi(t)$ denotes the shaping pulse in duration T satisfying $\int_T \varphi^2(t)dt = 1$. Due to the orthogonality of pilot signals transmitted by different RF chains, we get

$$\int_{M_t T} p_i(t)p_j(t)dt = \begin{cases} \frac{E}{M_t}, & i = j \\ 0, & i \neq j \end{cases} \tag{4}$$

To distinguish between large-scale fading and small-scale fading, we consider the frame structure shown in Fig.2. As we can see, each frame consists of N resource blocks. Within a single resource block, the mm-wave channel is set to remain constant; between the different resource blocks, the gain of each path in the channel will change, but the transmit and arrival angles of the path remain constant. The pilot signal, betokened as $p_m(q,t) = p_m(t-(q-1)T_b)$ is sent by the m^{th} RF chain in the q^{th} block, where $q = 1, \ldots, N$ and $m = 1, \ldots, M_t$. Here, T_b denotes the block duration.

Based on the above discussion, the output of the receive beamformer can be expressed as

$$\mathbf{y}(q,t) = \mathbf{W}^H\mathbf{H}(q)\mathbf{F}\mathbf{p}(q,t) + \mathbf{W}^H\mathbf{n}(q,t) \in \mathbb{C}^{M_r} \tag{5}$$

where $\mathbf{p}(q,t) = \left[p_1(q,t), \ldots, p_{M_t}(q,t)\right]^T$ is the pilot signal vector and $\mathbf{n}(q,t)$ represents the i.i.d. Gaussian noise.

According to (5), the received signal expression contains the analog logarithmic beamformers $\mathbf{W}$ and $\mathbf{F}$, which means that channel estimation performanc is severely affected by the beamforming matrix. In the following section, spatial spectrum analysis and system simulations in the beamspace are combined with the DFT beamformer. The specific expression of the DFT beamformer is

$$\begin{aligned} \mathbf{F} &= \left[\mathbf{a}_t\left(\hat{\phi}_1\right)\mathbf{a}_t\left(\hat{\phi}_2\right)\ldots\mathbf{a}_t\left(\hat{\phi}_{M_t}\right)\right] \in \mathbb{C}^{N_t\times M_t} \\ \mathbf{W} &= \left[\mathbf{a}_r\left(\hat{\theta}_1\right)\mathbf{a}_r\left(\hat{\theta}_2\right)\ldots\mathbf{a}_r\left(\hat{\theta}_{M_r}\right)\right] \in \mathbb{C}^{N_r\times M_r} \end{aligned} \tag{6}$$

where

$$\begin{aligned} \hat{\phi}_i &= \hat{\phi}_1 + \frac{2}{N_t}(i-1), i = 1, \ldots, M_t, \hat{\phi}_1 \in [-1, 1] \\ \hat{\theta}_j &= \hat{\theta}_1 + \frac{2}{N_r}(j-1), j = 1, \ldots, M_r, \hat{\theta}_1 \in [-1, 1] \end{aligned} \tag{7}$$

As shown in Fig.2, we use the 2-D BMODE algorithm to estimate the path direction $\{(\phi_k, \theta_k)\}_{k=1}^K$, which consists of N fading blocks. The 2-D BMODE algorithm adopted is not a simple extension of its elemental space counterpart due to the existence of beamforming. As described in [17], the unsuitable beamformers may cause spectral ambiguity, making it difficult to uniquely determine the path angle. The path direction estimation will then serve as the basis for estimating the path gains in each block. Specifically, knowing the path direction, we can use the LS algorithm to estimate

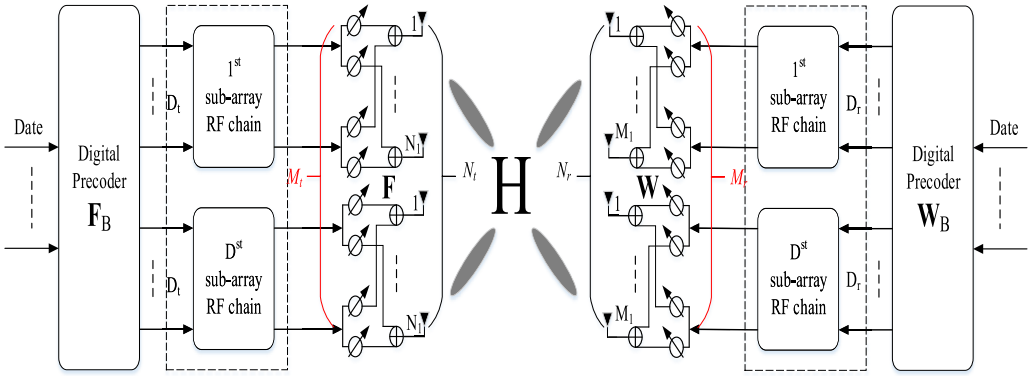

FIGURE 1. A mm-wave communication system employing hybrid analog/digital beamforming.

the path gain $\{\alpha_k(q)\}_{k=1}^K$, and then obtain the entire channel matrix $\mathbf{H}(q), q = 1, \ldots, N$.

In the condition of the orthogonality of the pilot waveforms, we apply matched-filtering to the received signal $\mathbf{y}(q,t)$ in (5) to obtain

$$\begin{aligned}\mathbf{y}_m(q) &= \int_{M_t T} \mathbf{y}(q,t) p_m(q,t) dt, \quad m = 1, \ldots, M_t \\ &= \frac{E}{M_t} \mathbf{W}^H \mathbf{H}(q) \mathbf{F}_{[:,m]} + \mathbf{n}_m(q) \end{aligned} \tag{8}$$

where we assume that the columns of $\mathbf{W}$ are orthogonal, so we have $\mathbf{n}_m(q) = \mathbf{W}^H \int_T \mathbf{n}(q,t) p_m(q,t) dt \sim \mathcal{CN}(\mathbf{0}, \sigma^2 \mathbf{I}_{\mathbf{M_r}})$. Substituting (1) into (8), we get

$$\begin{aligned}\mathbf{y}_m(q) &= \frac{E}{M_t} \mathbf{W}^H \sum_{k=1}^K \alpha_k(q) \mathbf{a}_r(\theta_k) \mathbf{a}_t^H(\phi_k) \mathbf{F}_{[:,m]} + \mathbf{n}_m(q) \\ &= \frac{E}{M_t} \sum_{k=1}^K \left(\mathbf{F}_{[:,m]}^H \mathbf{a}_t(\phi_k)\right)^* \mathbf{W}^H \mathbf{a}_r(\theta_k) \alpha_k(q) + \mathbf{n}_m(q) \\ &= \frac{E}{M_t} \Big[\left(\mathbf{F}_{[:,m]}^H \mathbf{a}_t(\phi_1)\right)^* \mathbf{W}^H \mathbf{a}_r(\theta_1) \cdots \\ &\quad \left(\mathbf{F}_{[:,m]}^H \mathbf{a}_t(\phi_K)\right) \mathbf{W}^H \mathbf{a}_r(\theta_K) \Big] \boldsymbol{\alpha}(q) + \mathbf{n}_m(q) \\ &= \frac{E}{M_t} \left(\mathbf{F}_{[:,m]}^H \mathbf{A}_T\right)^* \odot \left(\mathbf{W}^H \mathbf{A}_R\right) \boldsymbol{\alpha}(q) + \mathbf{n}_m(q) \end{aligned} \tag{9}$$

where $\boldsymbol{\alpha}(q) = [\alpha_1(q) \ldots \alpha_K(q)]^T$. If we stack all the M_t vectors in a column, we get the $M_t M_r \times 1$ measurement vector

$$\begin{aligned}\mathbf{y}(q) &= \left[\mathbf{y}_1(q)^T \ldots \mathbf{y}_{M_t}(q)^T\right]^T \\ &= \frac{E}{M_t} \begin{bmatrix} \left(\mathbf{F}_{[:,1]}^H \mathbf{A}_T\right)^* \\ \vdots \\ \left(\mathbf{F}_{[:,M_t]}^H \mathbf{A}_T\right)^* \end{bmatrix} \odot \left(\mathbf{W}^H \mathbf{A}_R\right) \boldsymbol{\alpha}(q) + \mathbf{n}(q) \\ &= \frac{E}{M_t} \underbrace{\left(\mathbf{F}^H \mathbf{A}_T\right)^* \odot \left(\mathbf{W}^H \mathbf{A}_R\right)}_{\mathbf{C}} \boldsymbol{\alpha}(q) + \mathbf{n}(q) \end{aligned} \tag{10}$$

where $\mathbf{n}(q) = \left[\mathbf{n}_1(q)^T, \ldots, \mathbf{n}_{M_t}(q)^T\right]^T$ and $\mathbf{C}$ is the $M_t M_r \times K$ direction matrix. The k^{th} column of $\mathbf{C}$ can be expressed as $\mathbf{c}(\phi_k, \theta_k)$, where the function $\mathbf{c}(\phi, \theta)$ is defined as

$$\mathbf{c}(\phi, \theta) = \left(\mathbf{F}^H \mathbf{a}_t(\phi)\right) \otimes \left(\mathbf{W}^H \mathbf{a}_r(\theta)\right) \tag{11}$$

Without loss of generality, we employ the measurement vectors from N previously collected blocks to capture the covariance matrix

$$\mathbf{R}_y \triangleq \mathbb{E}\left\{\mathbf{y}(q)\mathbf{y}(q)^H\right\} \simeq \widehat{\mathbf{R}}_y \triangleq \frac{1}{N} \sum_{q=1}^N \mathbf{y}(q)\mathbf{y}(q)^H \tag{12}$$

This is the basis of the proposed algorithm. The 2-D BMODE algorithm is a fast implementation to solve multidimensional nonlinear optimization problems, requiring signal subspace and noise subspace to come to fruition. Therefore, it is necessary to make a brief review of the covariance matrix of the received signal.

B. COVARIANCE MATRIX OF RECEIVED SIGNAL

The eigenvalue decomposition of covariance matrix is the crux of the proposed algorithm. Therefore, we should first form the sample covariance matrix. Substituting (10) into (12), we have

$$\begin{aligned}\mathbf{R}_y &= \mathbf{C}\mathbb{E}\left\{\boldsymbol{\alpha}(q)\boldsymbol{\alpha}(q)^H\right\} \mathbf{C}^H + \sigma^2 \mathbf{I}_{M_t M_r} \\ &= \underbrace{\mathbf{C}\Lambda\mathbf{C}^H}_{\mathbf{R}_x} + \sigma^2 \mathbf{I}_{M_t M_r} \end{aligned} \tag{13}$$

Assuming $\mathbf{C}$ is a full-rank column matrix, the eigenvalue decomposition of $\mathbf{R}_x$ is expressed as

$$\mathbf{R}_x = \mathbf{U}\text{diag}\left\{\eta_1, \eta_2, \ldots, \eta_{M_t M_r}\right\} \mathbf{U}^H \tag{14}$$

where $\{\eta_i\}_{i=1}^{M_t M_r}$ represent eigenvalues of $\mathbf{R}_x$, sorted in descending order. We establish $\text{rank}(\mathbf{R}_x) = K$ due to $\text{rank}(\mathbf{C}) = K$. Thus

$$\begin{cases} \eta_i > 0, & \text{for } i \le K \\ \eta_i = 0, & \text{for } i > K \end{cases} \tag{15}$$

According to (13), it is obvious that $\mathbf{R}_y$ has eigenvalues $\left\{\eta_i' = \eta_i + \sigma^2\right\}_{i=1}^{M_t M_r}$ and the same eigenvectors as $\mathbf{R}_x$. So the

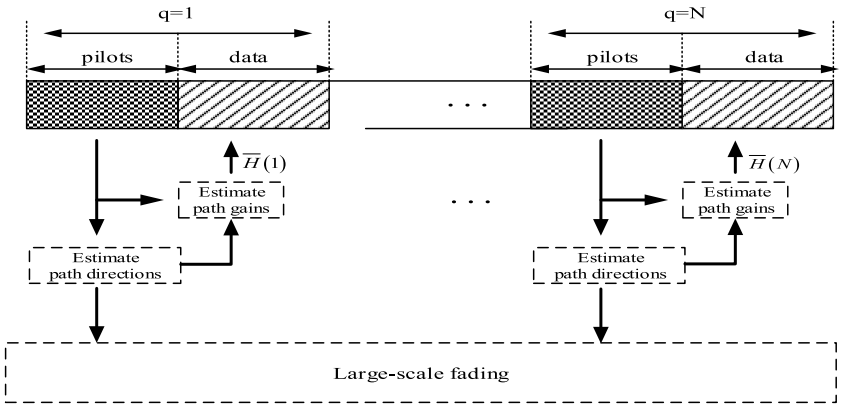

FIGURE 2. The framework of proposed mm-wave channel estimator.

eigenvalue decomposition of $\mathbf{R}_y$ can be written as

$$\begin{aligned}\mathbf{R}_y &= \mathbf{U}\,\mathrm{diag}\left\{\eta_1', \eta_2', \ldots, \eta_{M_tM_r}'\right\}\mathbf{U}^H \\ &= \mathbf{U}_s\boldsymbol{\Sigma}_s\mathbf{U}_s^H + \mathbf{U}_n\boldsymbol{\Sigma}_n\mathbf{U}_n^H\end{aligned} \tag{16}$$

where $\eta_i' = \sigma^2$ for $i > K$, as indicated by (15). Then the matrix $\mathbf{U}$ can be partitioned into $\mathbf{U} = [\mathbf{U}_s \mid \mathbf{U}_n]$, where $\mathbf{U}_s$ and $\mathbf{U}_n$ represent the signal and noise subspace. The columns in $\mathbf{U}_n \in \mathbb{C}^{M_tM_r\times(M_tM_r-K)}$ are the eigenvectors corresponding to the eigenvalue σ^2. Note that $\mathbf{U}_n$ in (16) can be estimated by performing an eigenvalue decomposition of the estimated sample covariance matrix $\widehat{\mathbf{R}}_y$ defined in (12). Here, it is assumed that the path number K is known.

C. 2-D BMODE FOR DOA ESTIMATION

The MODE algorithm is an improvement of the Iterative Quadratic Maximum Likelihood (IQML) algorithm and an implementation of the Maximum Likelihood(ML) algorithm. Its biggest advantage is that the computational cost is moderate and much smaller than the IQML algorithm. For simplicity of analysis, we use $\mathbf{A}$ to substitute $\left(\mathbf{W}^H\mathbf{A}_R\right)$ and $\mathbf{B}$ to substitute $\left(\mathbf{F}^H\mathbf{A}_T\right)^*$ in the following.

Initially, we attempt to define two coefficient vectors, $\mathbf{a} = [a_0, a_1, \cdots, a_K]^T$ and $\mathbf{b} = [b_0, b_1, \cdots, b_K]^T$. These coefficients are constructed similarly to two polynomials of the following form

$$\sum_{i=0}^{K} c_i z^{K-i} = c_0 \prod_{i=1}^{K}\left(z - e^{j\pi\sin\psi_i}\right), \quad c_0 \neq 0 \tag{17}$$

where $c_i \in \{a_i, b_i\}$ and $\psi_i \in \{\theta_i, \phi_i\}$ correspondingly. If we introduce the set

$$\mathbb{L} = \left\{\{c_i\} \mid \mathcal{C}(z) = \sum_{i=0}^{K} c_i z^{K-i} \neq 0 \text{ for } |z| \neq 1\right\} \tag{18}$$

it can be seen that the mapping from $\{\psi_i\} \in \mathbb{R}$ to $\{c_i\} \in \mathbb{L}$ is one-to-one, provided that we eliminate the non-uniqueness implied by the introduction of $c_0 \neq 1$.

Let $\mathbf{G_a} \in \mathbb{C}^{N_r\times(N_r-K)}$ and $\mathbf{G_b} \in \mathbb{C}^{N_t\times(N_t-K)}$, for $\mathbf{a}$ and $\mathbf{b}$, respectively, be with the following Toeplitz form

$$\mathbf{G}_{\mathbf{c}}^H = \begin{bmatrix} c_K & \cdots & c_1 & c_0 & \cdots & 0 \\ 0 & \ddots & \ddots & \ddots & \ddots & 0 \\ 0 & \cdots & c_K & \cdots & c_1 & c_0 \end{bmatrix}, \quad \mathbf{c} \in \{\mathbf{a}, \mathbf{b}\} \tag{19}$$

It is noticed that rank $\{\mathbf{G_a}\} = N_r - K$, rank $\{\mathbf{G_b}\} = N_t - K$, and

$$\mathbf{G}_{\mathbf{b}}^H\mathbf{A}_T = \mathbf{G}_{\mathbf{a}}^H\mathbf{A}_R = \mathbf{0} \tag{20}$$

Let

$$\mathbf{Z}_{\mathrm{a}} = \mathbf{W}^{-1}\mathbf{G_a} \tag{21}$$

then

$$\mathbf{Z}_{\mathrm{a}}^H\mathbf{A} = \mathbf{Z}_{\mathrm{a}}^H\left(\mathbf{W}^H\mathbf{A}_R\right) = \mathbf{G}_{\mathbf{a}}^H\mathbf{A}_R = \mathbf{0} \tag{22}$$

Therefore, based on the above relationship, we can derive the following equation, which can be used to estimate all DOA information.

$$\left(\mathbf{I}_{M_t} \otimes \mathbf{Z}_{\mathrm{a}}\right)^H(\mathbf{B} \odot \mathbf{A}) = \mathbf{B} \odot \left(\mathbf{Z}_{\mathrm{a}}^H\mathbf{A}\right) = \mathbf{0} \tag{23}$$

where we make use of the properties of the Kronecker product.

Let

$$\mathbf{V} = \mathbf{I}_{M_t} \otimes \mathbf{Z}_{\mathrm{a}} \tag{24}$$

$$\mathbf{R} = \left(\mathbf{V}^H\mathbf{V}\right)^{-1} \tag{25}$$

Then the ML algorithm can be simplified as

$$\min \boldsymbol{F}_R(\mathbf{a}) = \min_{\boldsymbol{\theta}, s_i} \mathrm{tr}\left[\mathbf{U}_{\mathrm{s}}^H\mathbf{V}\mathbf{R}\mathbf{V}^H\mathbf{U}_{\mathrm{s}}\right]\left(\Sigma_{\mathrm{s}} - \sigma^2\mathbf{I}\right) \tag{26}$$

where $\mathbf{U}_{\mathrm{s}}$, Σ_{s} and σ^2 can be acquired from (16). Iterating Constantly (26), the angle $\left\{\bar{\theta}_k\right\}_{k=1}^K$ is obtained when c_i converges. The process is summarized in Algorithm 1.

TABLE 1. Summary of the 2-D BMODE approach.

Algorithm 1 2-D BMODE Algorithm

1: The data covariance matrix is obtained by (12) from the received data of the array

2: Determine the initial value of $\mathbf{a}$

3: Using formula (25) to determine the matrix $\mathbf{R}^{1/2}$, $\mathbf{U}_{\mathrm{s}}\left(\mathbf{\Sigma}_{\mathrm{s}}-\sigma^2\mathbf{I}\right)^{1/2}=\left[\begin{array}{ccc}\tilde{\mathbf{e}}_1 & \cdots & \tilde{\mathbf{e}}_N\end{array}\right]$, $\mathbf{V}^H\tilde{\mathbf{e}}_k=\widetilde{\mathbf{E}}_k\mathbf{a}$ to determine the matrix $\tilde{\mathbf{e}}_k$ and $\widetilde{\mathbf{E}}_k$

4: The matrix $\boldsymbol{H}$ is determined by formula $\boldsymbol{H}=\left[\begin{array}{c}\mathbf{R}^{1/2}\widetilde{\mathbf{E}}_1\\ \vdots \\ \mathbf{R}^{1/2}\widetilde{\mathbf{E}}_{\mathrm{N}}\end{array}\right]$, and the matrix $\boldsymbol{O}$ is obtained by formula

$$\begin{aligned}\boldsymbol{F}_R(\mathbf{a}) &= \left\|\left[\begin{array}{ccc}\boldsymbol{H}_{1\mathrm{r}}+(\boldsymbol{H}_2\boldsymbol{J})_{\mathrm{r}} & (\boldsymbol{H}_2\boldsymbol{J})_i-\boldsymbol{H}_{1i} & \boldsymbol{h}_{\mathrm{r}}\\ \boldsymbol{H}_{1\mathrm{i}}+(\boldsymbol{H}_2\boldsymbol{J})_i & \boldsymbol{H}_{1r}-(\boldsymbol{H}_2\boldsymbol{J})_{\mathrm{r}} & \boldsymbol{h}_{\mathrm{i}}\end{array}\right]\left[\begin{array}{c}\boldsymbol{\beta}_r\\ \boldsymbol{\beta}_{\mathrm{i}}\\ \mu\end{array}\right]\right\|^2\\ &= \|\boldsymbol{O}\boldsymbol{\rho}\|^2, \text{ where } \boldsymbol{\rho}=\left[\begin{array}{ccc}\boldsymbol{\beta}_{\mathrm{r}} & \boldsymbol{\beta}_i & \mu\end{array}\right]^T\end{aligned}$$

5: Determine the vector $\boldsymbol{\beta}$ and update the vector $\mathbf{a}$

6: If the vector $\mathbf{a}$ converges, it stops, otherwise repeat step 3

$\boldsymbol{\beta}$ can be received by [22]

D. RD-MUSIC ALGORITHM

Once all DOAs are obtained, we can use the RD-MUSIC algorithm [23] to divide the 2-D algorithm into two optimization problems.

$$\min_{\theta}\mathbf{B}(\phi)^H\mathbf{Q}(\theta)\mathbf{B}(\phi),\qquad \text{s.t. } \mathbf{e}^H\mathbf{A}_T(\phi)=1 \tag{27}$$

where

$$\mathbf{Q}(\theta)=\left[\mathbf{I}_{M_t}\otimes\mathbf{A}(\theta)\right]^H\mathbf{U}_n\mathbf{U}_n^H\left[\mathbf{I}_{M_t}\otimes\mathbf{A}(\theta)\right] \tag{28}$$

and $\mathbf{e}=[1,0,\cdots,0]^T$. As mentioned earlier, $\mathbf{A}$ represents $\left(\mathbf{W}^H\mathbf{A}_R\right)$.

After that, we can further construct a Lagrange cost function

$$\mathcal{P}(\phi,\eta)=\mathbf{B}(\phi)^H\mathbf{Q}(\theta)\mathbf{B}(\phi)+\eta\left[1-\mathbf{e}^H\mathbf{A}_T(\phi)\right] \tag{29}$$

where η is the Lagrange multiplier. By setting the gradient of (29) with respect to $\mathbf{B}(\phi)$ equal to zero, we can obtain the estimated steering vectors for this cost function with nonsingular $\mathbf{Q}(\theta)$. According to the above, $\mathbf{B}(\phi)$ represents $\left(\mathbf{F}^H\mathbf{A}_T\right)^*$, thus, for each $\bar{\phi}_k$,

$$\mathbf{a}_t\left(\phi_k\right)=\left.\frac{\left(\mathbf{F}^*\mathbf{Q}\right)^{-1}\mathbf{e}}{\mathbf{e}^H\left(\mathbf{F}^*\mathbf{Q}\mathbf{F}^T\right)^{-1}\mathbf{e}}\right|_{\theta=\bar{\theta}_k},\quad k=1,2,\cdots,K \tag{30}$$

Inserting $\left\{\bar{\theta}_k\right\}_{k=1}^K$ into (30), we obtain K vectors $\hat{\mathbf{a}}_t\left(\phi_1\right),\hat{\mathbf{a}}_t\left(\phi_2\right),\ldots,\hat{\mathbf{a}}_t\left(\phi_K\right)$. Then, the estimated auto-paired DODs information can be obtained from the above steering vectors using the LS principle.

The transmit steering vector for ϕ_k is $\mathbf{a}_t\left(\phi_k\right)=\left[1,\exp\left(-j\pi\sin\phi_k\right),\ldots,\exp\left(-j\pi\left(N_t-1\right)\sin\phi_k\right)\right]^T$, and we get

$$\mathbf{g}_k=-angle\left(\mathbf{a}_t\left(\phi_k\right)\right) \tag{31}$$

where $angle(.)$ is to determine the phase angle of each element in the complex array. $\mathbf{g}_k=[0,\sin\phi_k,\ldots,(N_t-1)\sin\phi_k]^T$, and the LS principle is then applied to estimate $\sin\phi_k$. The normalization for the estimated vector $\hat{\mathbf{a}}_t\left(\phi_k\right)(k=1,2,\ldots,K)$ is primarily processed, and then the normalized sequence is processed to obtain $\hat{\mathbf{g}}_k$ according to (31). Now we apply the LS principle to estimate transmit angle ϕ_k. LS fitting is

$$\min_{c_k}\left\|\mathbf{P}\mathbf{c}_k-\hat{\mathbf{g}}_k\right\|_F^2 \tag{32}$$

where $\mathbf{c}_k=[c_{k0},c_{k1}]^T\in R^{2\times1}$ is an unknown parameter vector, and c_{k1} is the estimated value of $\sin\phi_k$; c_{k0} is the other estimation parameter. $\mathbf{P}$ is

$$\mathbf{P}=\left(\begin{array}{cc}1 & 0\\ 1 & 1\\ \vdots & \vdots\\ 1 & M-1\end{array}\right) \tag{33}$$

The LS solution for $\mathbf{c}_k$ is $\left[\hat{c}_{k0},\hat{c}_{k1}\right]^T=\left(\mathbf{P}^T\mathbf{P}\right)^{-1}\mathbf{P}^T\hat{\mathbf{g}}_k$, and the transmit angle ϕ_k is estimated through

$$\hat{\phi}_k=\sin^{-1}\left(\hat{c}_{k1}\right) \tag{34}$$

By this point, joint DOAs and DODs estimation has already been acquired. Unfortunately, theoretical analysis indicates that when the covariance matrix of gains exhibits rank deficiency, the 2-D BMODE algorithm struggles to accurately distinguish DODs due to spectrum ambiguity. In the next stage, we will leverage oblique projecting to obtain comprehensive information about the mm-wave channel. Without loss of generality, we assume that it generates a total of K clusters. Among them, there are K_1 clusters with distinct gain values. Additionally, there may exist Q groups of clusters with identical gain values. $l=1,2,\cdots,L_q,q=1,2,\cdots,Q$. For convenience, let $K_2=\sum_{q=1}^{Q}L_q$, then we have $K=K_1+K_2$. It is worth mentioning that the numbers of clusters K_1, K_2, and groups Q are also assumed to be known. Thus, Equation (10) can be rewritten as

$$\begin{aligned}\mathbf{y}(q)&=\frac{E}{M_t}\left(\mathbf{B}_d\odot\mathbf{A}_d\right)\boldsymbol{\alpha}_d(q)+\left(\mathbf{B}_s\odot\mathbf{A}_s\right)\boldsymbol{\alpha}_s(q)+\mathbf{n}(q)\\ &=\frac{E}{M_t}(\mathbf{B}\odot\mathbf{A})\boldsymbol{\alpha}(q)+\mathbf{n}(q)\end{aligned} \tag{35}$$

where $\mathbf{B}_d$, $\mathbf{A}_d$ and $\boldsymbol{\alpha_d}$ represent clusters with distinct gain values; $\mathbf{B}_s$, $\mathbf{A}_s$ and $\boldsymbol{\alpha_s}$ represent clusters with identical gain values.

E. OBLIQUE PROJECTING FOR DOD ESTIMATION

For DOD estimation of clusters with identical gain values, the contribution of clusters with distinct gains in $\mathbf{R}_y$ must to be eliminated. This can be realized through the so-called oblique projection (OP) technique.

An oblique projection [24] is a type of nonorthogonal projection, e.g., $\mathbf{P}_{\mathbf{D}_1\mathbf{D}_2}$, where its range is spanned by $\mathbf{D}_1$ and its null space is spanned by $\mathbf{D}_2$,

$$\mathbf{P}_{\mathbf{D}_1\mathbf{D}_2}=\mathbf{D}_1\left(\mathbf{D}_1^H\mathbf{P}_{\mathbf{D}_2}^{\perp}\mathbf{D}_1\right)^{-1}\mathbf{D}_1^H\mathbf{P}_{\mathbf{D}_2}^{\perp} \tag{36}$$

so that $\mathbf{P}_{\mathrm{D}_1\mathrm{D}_2}\mathbf{D}_1=\mathbf{D}_1$ and $\mathbf{P}_{\mathbf{D}_1\mathbf{D}_2}\mathbf{D}_2=\mathbf{0}$. In the scenario we discussed, if let $\mathbf{D}_1=\mathbf{B}_d\odot\mathbf{A}_d$ and $\mathbf{D}_2=\mathbf{B}_s\odot\mathbf{A}_s$, we can

construct a virtual observation matrix $\mathbf{Y}$ with only clusters with identical gain retaining, i.e.,

$$\begin{aligned}\mathbf{Y} &\triangleq \left(\mathbf{I}_{M_rM_t} - \mathbf{P}_{\mathbf{D}_1\mathbf{D}_2}\right)\left(\mathbf{R}_{\mathbf{y}} - \hat{\sigma}_n^2\mathbf{I}_{M_rM_t}\right)\left(\mathbf{I}_{M_rM_t} - \mathbf{P}_{\mathbf{D}_1\mathbf{D}_2}\right)^H \\ &= \left(\mathbf{B}_s \odot \mathbf{A}_s\right)\mathbf{R}_s\left(\mathbf{B}_s \odot \mathbf{A}_s\right)^H \\ &= \left(\mathbf{B}_s \odot \mathbf{A}_s\right)\mathbf{G}_s \end{aligned} \tag{37}$$

where $\hat{\sigma}_n^2 = \frac{1}{M_rM_t - K_1 - Q}\sum_{i=K_1+Q+1}^{M_rM_t}\eta_i$.

Therefore, the core problem is how to design a practical oblique projection. To our knowledge, the calculation of $\mathbf{P}_{\mathbf{D}_2}^{\perp}$ in (36) is unrealistic because $\mathbf{B}_s \odot \mathbf{A}_s$ is unknown. Reference [25] suggests that if we substitute $\mathbf{R}^{\dagger}$ for $\mathbf{P}_{\mathbf{D}_2}^{\perp}$, where $\mathbf{R}^{\dagger} = \mathbf{U_s}\Sigma_{\mathbf{s}}^{-1}\mathbf{U}_{\mathbf{s}}^H$, i.e., $\mathbf{P}_{\mathbf{D}_1\mathbf{D}_2} = \mathbf{D}_1\left(\mathbf{D}_1^H\mathbf{R}^{\dagger}\mathbf{D}_1\right)^{-1}\mathbf{D}_1^H\mathbf{R}^{\dagger}$, it then works [26], [27]. Nevertheless, the approximation usually causes confusion because the power and information of the clusters with identical gain values contributing to $\mathbf{U_s}$ are subtracted in $\mathbf{Y}$.

1) NEW OBLIQUE PROJECTOR

The essence of this new oblique projector lies in the estimated DOA information of the clusters with identical gain values, i.e., $\{\bar{\theta}_i\}_{i=K_1+1}^{K}$.

On account on these, a K_2-order polynomial with roots $\left\{e^{j\pi\sin\bar{\theta}_i}\right\}_{i=K_1+1}^{K}$ and $K_2 = K - K_1$ can be reconstructed. For convenience, the coefficients are defined by the vector

$$\mathbf{h} = \left[h_0, h_1, \cdots, h_{K_2}\right]^T \tag{38}$$

Similar to (19), a Toeplitz matrix $\mathbf{G_h} \in \mathbb{C}^{M_t\times(M_t-K_2)}$ can be used to help create oblique projections as it satisfies $\mathbf{G}_{\mathbf{h}}^H\mathbf{B}_s = \mathbf{0}$. If defining $\overline{\mathbf{G}} = \mathbf{G_h}\otimes\mathbf{I}_{M_r}$, then we have

$$\overline{\mathbf{G}}^H\mathbf{D}_2 = \overline{\mathbf{G}}^H\left(\mathbf{B}_s \odot \mathbf{A}_s\right) = \left(\mathbf{G}_{\mathbf{h}}^H\mathbf{B}_s\right)\odot\mathbf{A}_s = \mathbf{0} \tag{39}$$

In other words, it can allow us to substitute $\mathbf{P}_{\overline{\mathbf{G}}}$ for $\mathbf{P}_{\mathbf{D}_2}^{\perp}$ in (36), which creates an alternative to oblique projectors, i.e.,

$$\overline{\mathbf{P}}_{\mathbf{D}_1\mathbf{D}_2} = \mathbf{D}_1\left(\mathbf{D}_1^H\mathbf{P}_{\overline{\mathbf{G}}}\mathbf{D}_1\right)^{-1}\mathbf{D}_1^H\mathbf{P}_{\overline{\mathbf{G}}} \tag{40}$$

where $\mathbf{P}_{\overline{\mathbf{G}}} = \overline{\mathbf{G}}\left(\overline{\mathbf{G}}^H\overline{\mathbf{G}}\right)^{-1}\overline{\mathbf{G}}^H$. We can easily go over the attributes that $\overline{\mathbf{P}}_{\mathbf{D}_1\mathbf{D}_2}\mathbf{D}_1 = \mathbf{D}_1$ and $\overline{\mathbf{P}}_{\mathbf{D}_1\mathbf{D}_2}\mathbf{D}_2 = \mathbf{0}$. In this paper, the algorithm is called improved 2-D BMODE algorithm in which $\overline{\mathbf{P}}_{\mathbf{D}_1\mathbf{D}_2}$ takes the place of $\mathbf{P}_{\mathbf{D}_1\mathbf{D}_2}$.

F. FORWARD-BACKWARD SPATIAL SMOOTHING

Substituting (40) into (37), we can obtain the virtual observation Y. If $\mathbf{B}_s \odot \mathbf{A}_s$ is a full column rank matrix and Λ is a rank-deficient matrix due to equal gain, we must use the 2-D spatial smoothing technique. Define a series of selection matrices, $n = 1, 2, \cdots, N_t - Z_1 + 1$, $m = 1, 2, \cdots, N_r - Z_2 + 1$

$$\begin{aligned}\Gamma_{\mathrm{n,m}} = &\left[\mathbf{0}_{Z_1\times(n-1)}\mathbf{I}_{Z_1}\mathbf{0}_{Z_1\times(N_t-Z_1-n+1)}\right] \\ &\otimes\left[\mathbf{0}_{Z_2\times(m-1)}\mathbf{I}_{Z_2}\mathbf{0}_{Z_2\times(N_r-Z_2-m+1)}\right]\end{aligned} \tag{41}$$

where $Z_1 < N_t$ and $Z_2 < N_r$ indicate the length of receive and transmit subarrays, respectively. Let

$$\mathbf{J} = \left(\mathbf{F}^T\right)^{-1}\otimes\left(\mathbf{W}^H\right)^{-1} \tag{42}$$

$$\mathbf{Y_2} = \mathbf{JY} \tag{43}$$

Subsequently stacking $\Gamma_{\mathrm{n,m}}\mathbf{Y_2}$ as the following style

$$\begin{aligned}&\left[\Gamma_{1,1}\mathbf{Y_2}\cdots\Gamma_{1,N_r-Z_2+1}\mathbf{Y_2}\Gamma_{2,1}\mathbf{Y_2}\right. \\ &\qquad\left.\cdots\Gamma_{2,N_r-Z_2+1}\mathbf{Y_2}\cdots\Gamma_{N_t-Z_1+1,N_r-Z_2+1}\mathbf{Y_2}\right]\end{aligned}$$

it holds

$$\overline{\mathbf{Y}} \triangleq \left[\mathbf{B}_s^{(Z_1)}\odot\mathbf{A}_s^{(Z_2)}\right]\overline{\mathbf{G}}_s \tag{44}$$

Note that $\overline{\mathbf{G}}_s \in \mathbb{C}^{K_2\times(N_t-Z_1+1)(N_r-Z_2+1)N_tN_r}$ is a gain matrix that in turn decorrelates the rank-deficient $\mathbf{G}_s$, making it a full row rank matrix. Furthermore, similar to the traditional smoothing technique, the choices of Z_1 and Z_2 depend mainly on the number of the clusters with identical gain values.

Taking advantage of the noise subspace of $\overline{\mathbf{Y}}$, i.e., $\overline{\mathbf{U}}_{\mathbf{n}}$, we can obtain the estimated auto-paired transmit steering vectors for the gain matrix with identical gain values,

$$\bar{\mathbf{a}}_t\left(\phi_k\right) = \frac{\left(\overline{\mathbf{Q}}\right)^{-1}\bar{\mathbf{e}}}{\bar{\mathbf{e}}^H\left(\overline{\mathbf{Q}}\right)^{-1}\bar{\mathbf{e}}}, k = K_1+1, \cdots, K \tag{45}$$

where $\overline{\mathbf{Q}} = \left[\mathbf{I}_{Z_1}\otimes\overline{\mathbf{A}}(\theta)\right]^H\overline{\mathbf{U}}_{\mathbf{n}}\overline{\mathbf{U}}_{\mathbf{n}}^H\left[\mathbf{I}_{Z_1}\otimes\overline{\mathbf{A}}(\theta)\right]$ with $\overline{\mathbf{A}}(\theta) = \mathbf{A}^{(Z_2)}(\phi)$, and $\bar{\mathbf{e}} = \mathbf{e}^{(Z_2)}$.

G. LS ESTIMATION OF PATH GAINS

Once the path angles are estimated by the 2-D BMODE method, $\widehat{\mathbf{c}}(\phi,\theta)$ can be obtained from (11), forming the direction matrix $\widehat{\mathbf{C}}$. After that, the path gain in (10) can be determined using the LS method as

$$\hat{\boldsymbol{\alpha}}(q) = \frac{M_t}{E}\left(\widehat{\mathbf{C}}^H\widehat{\mathbf{C}}\right)^{-1}\widehat{\mathbf{C}}^H\mathbf{y}(q), q = 1, 2, \ldots, N \tag{46}$$

The channel matrix $\mathbf{H}(q)$ in (2) can be obtained by substituting AoDs, AoAs and the path gain achieved by the above discussion. It should be noted that the order of the elements in $\hat{\boldsymbol{\alpha}}(q)$ is determined by $\widehat{\mathbf{C}}$. Put differently, the k^{th} element in $\hat{\boldsymbol{\alpha}}(q)$ is the gain $\widehat{\mathbf{C}}$ of the path whose direction contributes to the k^{th} column. Eventually, in TABLE 2, the complete process of the proposed approach is summarized.

IV. COMPUTATIONAL COMPLEXITY

Now, we analyze the computational complexity of the 2-D BMODE method in detail. One flop is defined as one-time complex multiplication according to [28]. For easy comparison, we herein consider the RD-MUSIC + oblique projection + SS + RD-MUSIC algorithm, in which the discerning of clusters with distinct gain values is easily achieved by the angles concerning K_1 least spectrum peak or by calculating (29). The computational complexity is analyzed as follows: distinct

TABLE 2. Summary of complete process of the approach proposed.

Algorithm 2 complete process of angles and gains

1: Initialization: The noise covariance matrix $\sigma^2\mathbf{I}_{M_tM_r}$.
The number of paths K. $\widehat{\mathbf{R}}_y = \mathbf{0}$
Estimate the Path Directions
2: Form sample covariance and perform eigenvalue decomposition

$$\widehat{\mathbf{R}}_y = \frac{1}{N}\sum_{q=1}^{N}\mathbf{y}(q)\mathbf{y}(q)^H = [\mathbf{U}_s \mid \mathbf{U}_n]\,\mathrm{diag}\{\lambda_1, \lambda_2, \ldots, \lambda_{M_tM_r}\}[\mathbf{U}_s \mid \mathbf{U}_n]^H$$

where $\mathbf{U}_n$ consists of eigenvectors corresponding to the smallest $M_tM_r - K$ eigenvalues.
3: By continuously iterate (26), DOA$\{\bar{\theta}_k\}_{k=1}^{K}$ are obtained; DOD are seized by(30)and(32); when $\mathbf{\Lambda}_\alpha$ is non-full rank, use oblique projection and forward-backward spatial smoothing to receive valid DOD and DOA
4: Compute $\widehat{\mathbf{A}}_T = [\mathbf{a}_t(\phi_1)\ldots\mathbf{a}_t(\phi_K)]$, $\widehat{\mathbf{A}}_R = [\mathbf{a}_r(\theta_1)\ldots\mathbf{a}_r(\theta_K)]$, and $\widehat{\mathbf{C}}_{[:,k]} = \mathbf{c}(\phi_k, \theta_k), k = 1, \ldots, K$
Estimate the Block-Fading Channel
5: **for** $q = 1$ to N do
6: Estimate the instantaneous path gains $\hat{\alpha}(q)$ according to (46). Then the block channel is estimated as
$\widehat{\mathbf{H}}(q) = \widehat{\mathbf{A}}_R\,\mathrm{diag}(\hat{\boldsymbol{\alpha}}(q))\widehat{\mathbf{A}}_T^H$
7: **end for**

gain values corresponding to DOA and DOD estimation require $\mathcal{O}\left\{{M_r}^3{M_t}^3 + \left(K^2 + M_r - K\right)\Gamma + (k_1 + k) \times \left[\left({M_r}^2{M_t}^2 + {M_r}^2\right)(M_rM_t - k_1 - Q) + {M_r}^3\right]\right\}$, where Γ is the number of iterations; oblique projection and SS require $\mathcal{O}\left\{3M_t^3M_r^3 + 3K_1M_t^2M_r^2 + 3K_1^2M_tM_r + 2K_1^3\right\}$. Especially, oblique projection and SS required in the improved 2-D BMODE approach require $\mathcal{O}\left\{M_r^3(M_t - K_2)\left[M_t^2 + 2M_t(M_t - K_2) + (M_t - K_2)^2\right] + 3M_t^3M_r^3 + 2K_1M_t^2M_r^2 + 2K_1^2M_tM_r + K_1^3\right\}$. The clusters with identical gain values estimation require $\mathcal{O}\left\{Z_1^3Z_2^3 + K_2\left[Z_2^2(Z_1 + 1)(Z_1Z_2 - K_2) + Z_2^3\right]\right\}$.

For the 2-D BMUSIC method, multi-dimensional search requires $\mathcal{O}\left(M_t^2M_r^2G_\theta G_\phi\right)$, where G_θ and G_ϕ is the total searching number in the whole angle domain. Oblique projection and SS is similar to 2-D BMODE method. The clusters with identical gain values estimation require $\mathcal{O}\left\{Z_1^3Z_2^3 + G_\phi G_\theta\left[(N_t - Z_1 + 1)^2(N_r - Z_2 + 1)^2\right]\right\}$. It is evident that the difference in complexity between these two methods increases with the angular resolution. Consequently, the 2-D BMODE method has significant advantages in reducing the cost of the calculation. The computational complexity of several channel estimation methods discussed above detailed in TABLE 3.

If taking some typical values of parameters into account, e.g., $N_t = M_t = 8$, $N_r = M_r = 16$, $K = 4$, $K_1 = 2$, $Q = 14$, $K_2 = 2$, $G_\phi = G_\theta = 90°/0.1°$, $Z_1 = 5$, $Z_2 = 13$. Through meticulous calculations, we can observe that 2-D BMODE has a computational complexity of $\mathcal{O}\left\{1.06 \times 10^7\right\}$ and its improved version has a computational complexity of $\mathcal{O}\left\{1.54 \times 10^7\right\}$, whereas the compared one is of $\mathcal{O}\left\{1.35 \times 10^{10}\right\}$, which significantly increases the complexity with the angular resolution. In other words, our proposed method has a substantial advantage in computational efficiency.

TABLE 3. Computational complexities of the proposed and comparative algorithms.

Algorithm	Complexity
2-D MUSIC	$4M_t^3M_r^3 + G_\phi G_\theta M_t^2M_r^2 + Z_1^3Z_2^3 + 3K_1M_t^2N_r^2$ $+G_\phi G_\theta[(N_t - Z_1 + 1)^2 \times (N_r - Z_2 + 1)^2]$ $+2K_1^3 + 3K_1^2M_tN_r$
2-D BMODE	$4M_t^3M_r^3 + (K^2 + M_r - K)\Gamma + Z_1^3Z_2^3 + 2K_1^3$ $+(K_1 + K)[(M_r^2M_t + M_r^2)(M_tM_r - K_1 - Q)$ $+M_r^3] + K_2[Z_2^2(Z_1 + 1)(Z_1Z_2 - K_2) + Z_2^3]$ $+K_1M_tM_r(3M_tM_r + 3K_1)$
IMP 2-D BMODE	$4M_t^3M_r^3 + (K^2 + M_r - K)\Gamma + Z_1^3Z_2^3 + K_1^3$ $+(K_1 + K)[(M_r^2M_t + M_r^2)(M_tM_r - K_1 - Q)$ $+M_r^3] + K_2[Z_2^2(Z_1 + 1)(Z_1Z_2 - K_2) + Z_2^3]$ $+M_r^3(M_t - K_2)[M_t^2 + 2M_t(M_t - K_2)$ $+(M_t - K_2)^2] + 2K_1M_tM_r(M_tM_r + K_1)$

V. SIMULATION RESULTS

The channel estimation performance of the mm-wave channel modeled by ray-tracing is investigated through Monte Carlo simulation.

In this section, we elaborate on the performance of the proposed channel estimator through computer simulation with the following parameters. The ULAs at the transmitter and receiver are equipped with $N_t = 8$ and $N_r = 16$ antenna elements, respectively. There are $M_t = 8$ RF chains at the transmitter and $M_r = 16$ RF chains at the receiver. The DFT beamformers defined in (6) are used in the simulations to avoid the beamspace spatial spectrum ambiguity effect. $\frac{E}{N_t\sigma^2}$ represents the signal-to-noise ratio (SNR). We compare the proposed 2-D BMODE method with the 2-D BMUSIC method in [17] to exhibit the channel estimation performance. All results are averaged over 100 frames with N = 40, and in all channel realizations, the path directions $\{(\phi_k, \theta_k)\}_{k=1}^{K}$ are kept fixed, so the variation is only caused by the path gains $\{\alpha_k(q)\}_{k=1}^{K}$. There are four sharp peaks in the spectrum of 2-D BMUSIC in Fig.3(a), while only two in Fig.3(b) because of rank deficiency where two fuzzy bumps cause failing to acquire complete DOAs and DODs. Fig.3(c) indicats the excellence of oblique projecting + spatial smoothing when the rank deficiency of $\mathbf{\Lambda}$ leads to spectrum ambiguity. In Fig.4, we show the channel estimation performance of different channel estimators when the covariance matrix of gain is full column rank. Dantzig selector(DS)-based estimator is mentioned in [29]. The normalized mean-squared error (NMSE) is defined as $E\left\{\|\widehat{\mathbf{H}} - \mathbf{H}\|_F^2/\|\mathbf{H}\|_F^2\right\}$, where $\widehat{\mathbf{H}}$ denotes the estimate of the channel. In Fig.4, the proposed 2-D BMODE approach performs nearly the same as the 2-D BMUSIC. Moreover, both the 2-D BMUSIC and 2-D BMODE methods outperform OMP and DS counterparts significantly. This is because these methods have a higher angular resolution.

In Fig.5, the channel estimator based on the improved 2-D BMODE method, which uses new oblique projector, is very close to the MUSIC+OP algorithm when the covariance matrix of gain is rank deficiency. The performance of the

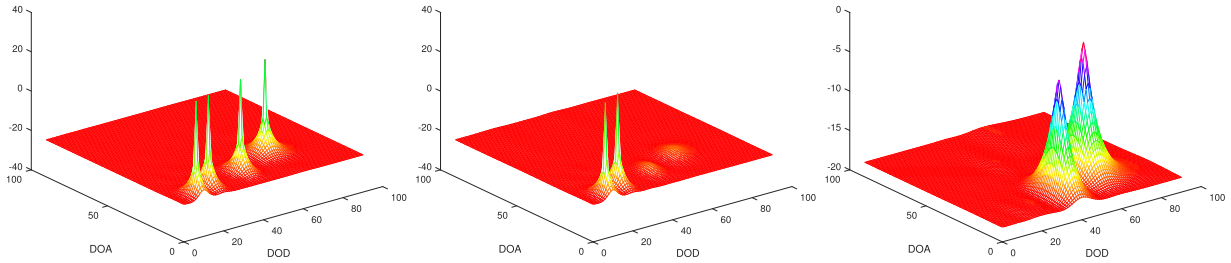

(a) Full column rank (b) Rank deficiency:distinct gain values (c) Rank deficiency:identical gain values

FIGURE 3. The 2-D beamspace direction spectrum.

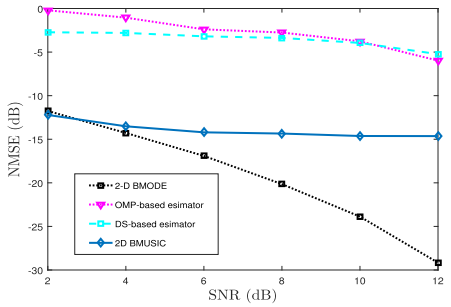

FIGURE 4. The performance comparison of channel estimator between several typical algorithms.

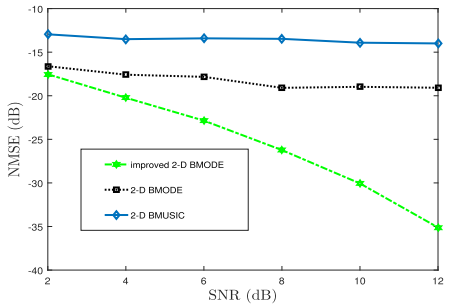

FIGURE 5. The NMSE performance as a function of SNR.

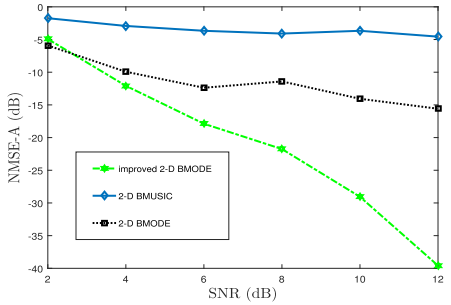

FIGURE 6. The NMSE of path angles as a function of SNR.

improved 2-D BMODE method is better than the 2-D BMODE method because it can reduce the error of $\mathbf{P}_{\mathbf{D}_2}^{\perp}$. In Fig.6, we show the MSE-A of the estimated path angles, which is defined as $\mathbb{E}\left\{\left(\phi_1-\tilde{\phi}_1\right)^2+\left(\theta_1-\tilde{\theta}_1\right)^2\right\}$. As we

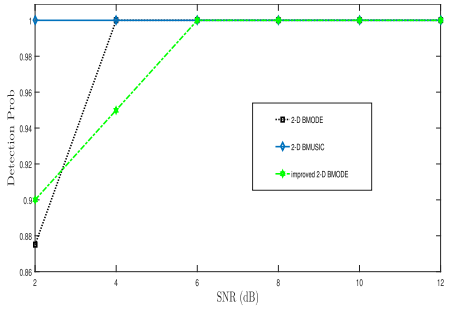

FIGURE 7. Path detection probability as a function of SNR.

can see in Fig.6, the proposed channel estimator shows considerable performance.

Next, we compare three types of channel estimation methods in terms of detection probability at SNRs ranging from 2 dB to 12 dB, where a successful detection is indicated by the deviation of estimated AoDs/AoAs being lower than the threshold Th. In the simulation, $Th = 0.04$, with 40 sample points and 100 snapshots.

As shown in Fig.7, it is apparent that the MUSIC+OP algorithm has a higher detection probability but requires higher computational cost. The method proposed in this paper can enhance detection probability by reducing iteration errors.

Therefore, both proposed methods can be considered as better choices than the existing competitors from the joint perspective of computational complexity and accuracy of angle estimation.

VI. CONCLUSION

We present a novel 2-D beamspace mm-wave channel estimation method that leverages the slow variation of path angles in comparision to path gain. The iterative 2-D BMODE algorithm significantly reduces the computational costs compared to the 2-D spectral peak search algorithm. The proposed algorithm's estimation accuracy can be enhanced by addressing the iteration error. Rank deficiency issues are mitigated through spatial smoothing technique and oblique projecting to acquire comprehensive channel information. DFT beamformers are employed to circumvent spectrum

ambiguity arising from pseudo pole. Once the angles are estimated, the LS method is applied to estimate fading gain in each block within the frame. Simulation results demonstrate that the proposed 2-D BMODE channel estimator achieves comparable performance with less time-consuming compared to existing methods. In the near future, our focus will be on addressing the system-level challenges of wideband mm-wave channel estimation.

REFERENCES

[1] Y. Sun, L. Zhang, G. Feng, B. Yang, B. Cao, and M. A. Imran, "Blockchain-enabled wireless Internet of Things: Performance analysis and optimal communication node deployment," *IEEE Internet Things J.*, vol. 6, no. 3, pp. 5791–5802, Jun. 2019.

[2] S. Rangan, T. S. Rappaport, and E. Erkip, "Millimeter-wave cellular wireless networks: Potentials and challenges," *Proc. IEEE*, vol. 102, no. 3, pp. 366–385, Mar. 2014.

[3] T. Bai, A. Alkhateeb, and R. W. Heath, "Coverage and capacity of millimeter-wave cellular networks," *IEEE Commun. Mag.*, vol. 52, no. 9, pp. 70–77, Sep. 2014.

[4] A. I. Sulyman, A. T. Nassar, M. K. Samimi, G. R. Maccartney, T. S. Rappaport, and A. Alsanie, "Radio propagation path loss models for 5G cellular networks in the 28 GHZ and 38 GHz millimeter-wave bands," *IEEE Commun. Mag.*, vol. 52, no. 9, pp. 78–86, Sep. 2014.

[5] C. H. Doan, S. Emami, D. A. Sobel, A. M. Niknejad, and R. W. Brodersen, "Design considerations for 60 GHz CMOS radios," *IEEE Commun. Mag.*, vol. 42, no. 12, pp. 132–140, Dec. 2004.

[6] A. Alkhateeb, O. E. Ayach, G. Leus, and R. W. Heath Jr., "Channel estimation and hybrid precoding for millimeter wave cellular systems," *IEEE J. Sel. Topics Signal Process.*, vol. 8, no. 5, pp. 831–846, Oct. 2014.

[7] J. Lee, G.-T. Gil, and Y. H. Lee, "Exploiting spatial sparsity for estimating channels of hybrid MIMO systems in millimeter wave communications," in *Proc. IEEE Global Commun. Conf.*, Dec. 2014, pp. 3326–3331.

[8] J. Mo, P. Schniter, N. G. Prelcic, and R. W. Heath, "Channel estimation in millimeter wave MIMO systems with one-bit quantization," in *Proc. 48th Asilomar Conf. Signals, Syst. Comput.*, Nov. 2014, pp. 957–961.

[9] Y. Xiao, Y. Wang, and W. Xiang, "Dimension-deficient channel estimation of hybrid beamforming based on compressive sensing," *IEEE Access*, vol. 7, pp. 13791–13798, 2019.

[10] M. Kokshoorn, H. Chen, P. Wang, Y. Li, and B. Vucetic, "Millimeter wave MIMO channel estimation using overlapped beam patterns and rate adaptation," *IEEE Trans. Signal Process.*, vol. 65, no. 3, pp. 601–616, Feb. 2017.

[11] A. Alkhateeb, O. El Ayach, G. Leus, and R. W. Heath, "Channel estimation and hybrid precoding for millimeter wave cellular systems," *IEEE J. Sel. Topics Signal Process.*, vol. 8, no. 5, pp. 831–846, Oct. 2014.

[12] Z. Xiao, P. Xia, and X.-G. Xia, "Channel estimation and hybrid precoding for millimeter-wave MIMO systems: A low-complexity overall solution," *IEEE Access*, vol. 5, pp. 16100–16110, 2017.

[13] Z. Gao, L. Dai, S. Han, C.-L. I, Z. Wang, and L. Hanzo, "Compressive sensing techniques for next-generation wireless communications," *IEEE Wireless Commun.*, vol. 25, no. 3, pp. 144–153, Jun. 2018.

[14] Y. Wu, Y. Gu, and Z. Wang, "Channel estimation for mmWave MIMO with transmitter hardware impairments," *IEEE Commun. Lett.*, vol. 22, no. 2, pp. 320–323, Feb. 2018.

[15] H. Chu, L. Zheng, and X. Wang, "Super-resolution mmWave channel estimation using atomic norm minimization," *IEEE J. Sel. Topics Signal Process.*, vol. 13, no. 6, pp. 1336–1347, Oct. 2019.

[16] P. Stoica and R. Moses, *Spectral Analysis of Signals*. Upper Saddle River, NJ, USA: Prentice-Hall, 2005.

[17] Z. Guo, X. Wang, and W. Heng, "Millimeter-wave channel estimation based on 2-D beamspace MUSIC method," *IEEE Trans. Wireless Commun.*, vol. 16, no. 8, pp. 5384–5394, Aug. 2017.

[18] A. Liao, Z. Gao, Y. Wu, H. Wang, and M.-S. Alouini, "2D unitary ESPRIT based super-resolution channel estimation for millimeter-wave massive MIMO with hybrid precoding," *IEEE Access*, vol. 5, pp. 24747–24757, 2017.

[19] S. Li, G. Cao, L. Jin, and H. Wu, "Channel estimation based on the PSS-MUSIC for millimeter-wave MIMO systems equipped with co-prime arrays," *EURASIP J. Wireless Commun. Netw.*, vol. 2020, no. 1, p. 17, Dec. 2020.

[20] P. Stoica and K. C. Sharman, "Maximum likelihood methods for direction-of-arrival estimation," *IEEE Trans. Acoust., Speech, Signal Process.*, vol. 38, no. 7, pp. 1132–1143, Jul. 1990.

[21] M. R. Akdeniz, Y. Liu, M. K. Samimi, S. Sun, S. Rangan, T. S. Rappaport, and E. Erkip, "Millimeter wave channel modeling and cellular capacity evaluation," *IEEE J. Sel. Areas Commun.*, vol. 32, no. 6, pp. 1164–1179, Jun. 2014.

[22] P. Stoica and K. C. Sharman, "Novel eigenanalysis method for direction estimation," *IEE Proc. F Radar Signal Process.*, vol. 137, no. 1, p. 19, 1990.

[23] X. Zhang, L. Xu, L. Xu, and D. Xu, "Direction of departure (DOD) and direction of arrival (DOA) estimation in MIMO radar with reduced-dimension MUSIC," *IEEE Commun. Lett.*, vol. 14, no. 12, pp. 1161–1163, Dec. 2010.

[24] R. T. Behrens and L. L. Scharf, "Signal processing applications of oblique projection operators," *IEEE Trans. Signal Process.*, vol. 42, no. 6, pp. 1413–1424, Jun. 1994.

[25] M. L. McCloud and L. L. Scharf, "A new subspace identification algorithm for high-resolution DOA estimation," *IEEE Trans. Antennas Propag.*, vol. 50, no. 10, pp. 1382–1390, Oct. 2002.

[26] X. Xu, Z. Ye, and J. Peng, "Method of direction-of-arrival estimation for uncorrelated, partially correlated and coherent sources," *IET Microw., Antennas Propag.*, vol. 1, no. 4, p. 949, 2007.

[27] X. Xu, Z. Ye, Y. Zhang, and C. Chang, "A deflation approach to direction of arrival estimation for symmetric uniform linear array," *IEEE Antennas Wireless Propag. Lett.*, vol. 5, pp. 486–489, 2006.

[28] G. Golub and C. V. Loan, *Matrix Computation*, 3rd ed. Baltimore, MD, USA: JHU Press, 2013.

[29] W. U. Bajwa, J. Haupt, A. M. Sayeed, and R. Nowak, "Compressed channel sensing: A new approach to estimating sparse multipath channels," *Proc. IEEE*, vol. 98, no. 6, pp. 1058–1076, Jun. 2010.

LI HOU was born in Nanking, in 1991. He received the B.S. degree from the Hefei University of Technology, China, in 2014, and the M.S. degree from Southeast University, China, in 2017, where he is currently pursuing the Ph.D. degree.

His research interests include statistical signal processing and its applications in wireless communications and cyber-physical systems.

JING WU received the B.S. degree in electronic science and technology and the M.S. degree in communication and information system from the Nanjing University of Posts and Telecommunications, China, in 2013 and 2016, respectively. She is currently pursuing the Ph.D. degree with the Department of Information Science and Engineering, Southeast University, China. Her research interests include statistical signal processing and its applications in wireless communications and cyber-physical systems.

WEI HENG (Member, IEEE) received the B.S. degree in information engineering from the Huazhong University of Science and Technology, in 1987, and the M.S. degree in signal and information processing and the Ph.D. degree in communications and information system from Southeast University, in 1990 and 1997, respectively. From 1997 to 2002, he was a Research Scholar with The Catholic University of America. Since 2002, he has been a Professor with the National Mobile Communications Research Laboratory, Southeast University. His research interests include mobile communications and signal processing.